Supplementary Figure S1

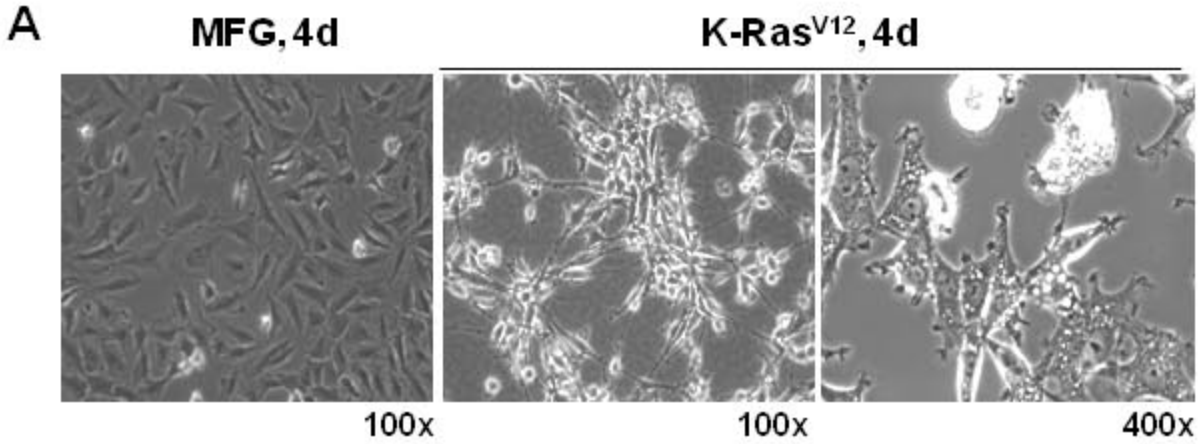

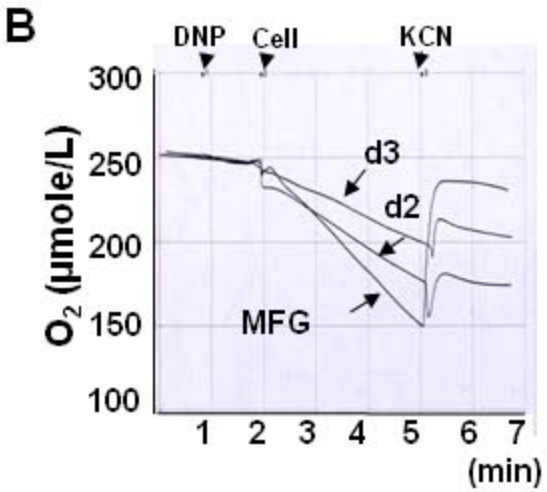

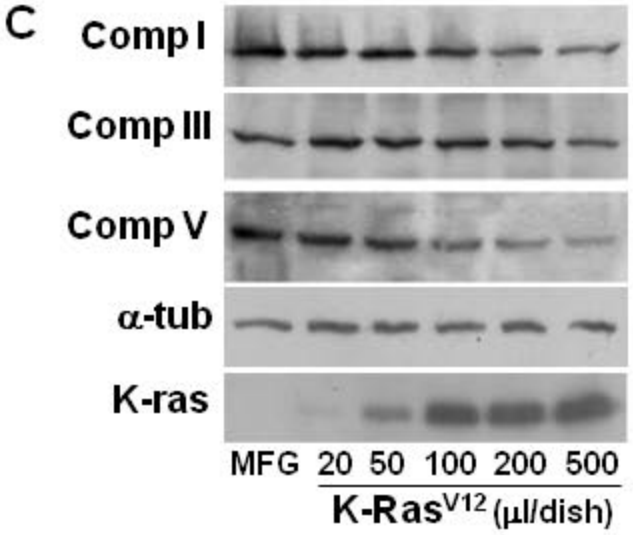

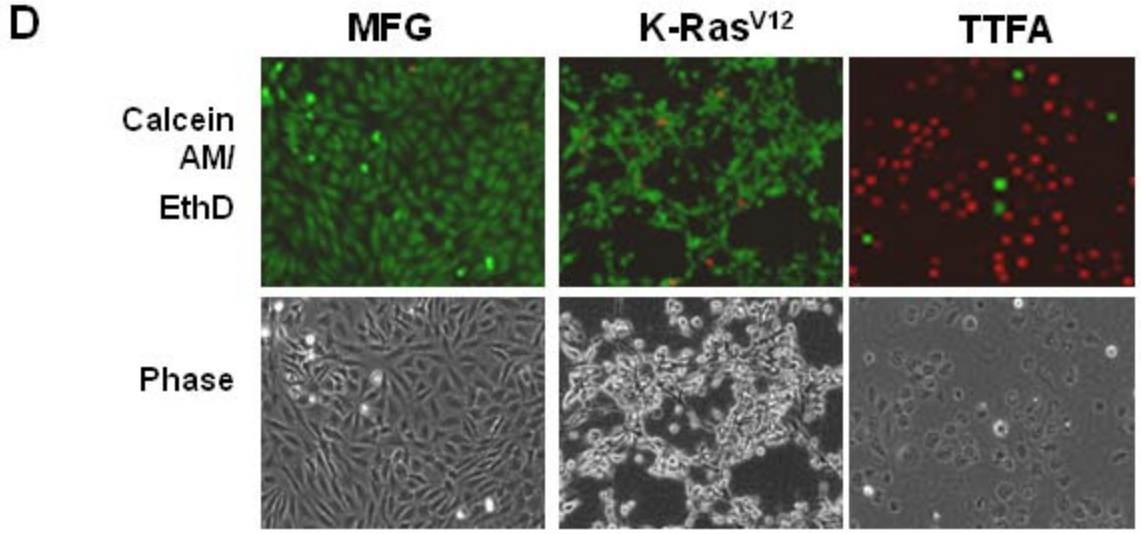

Supplementary Figure S2

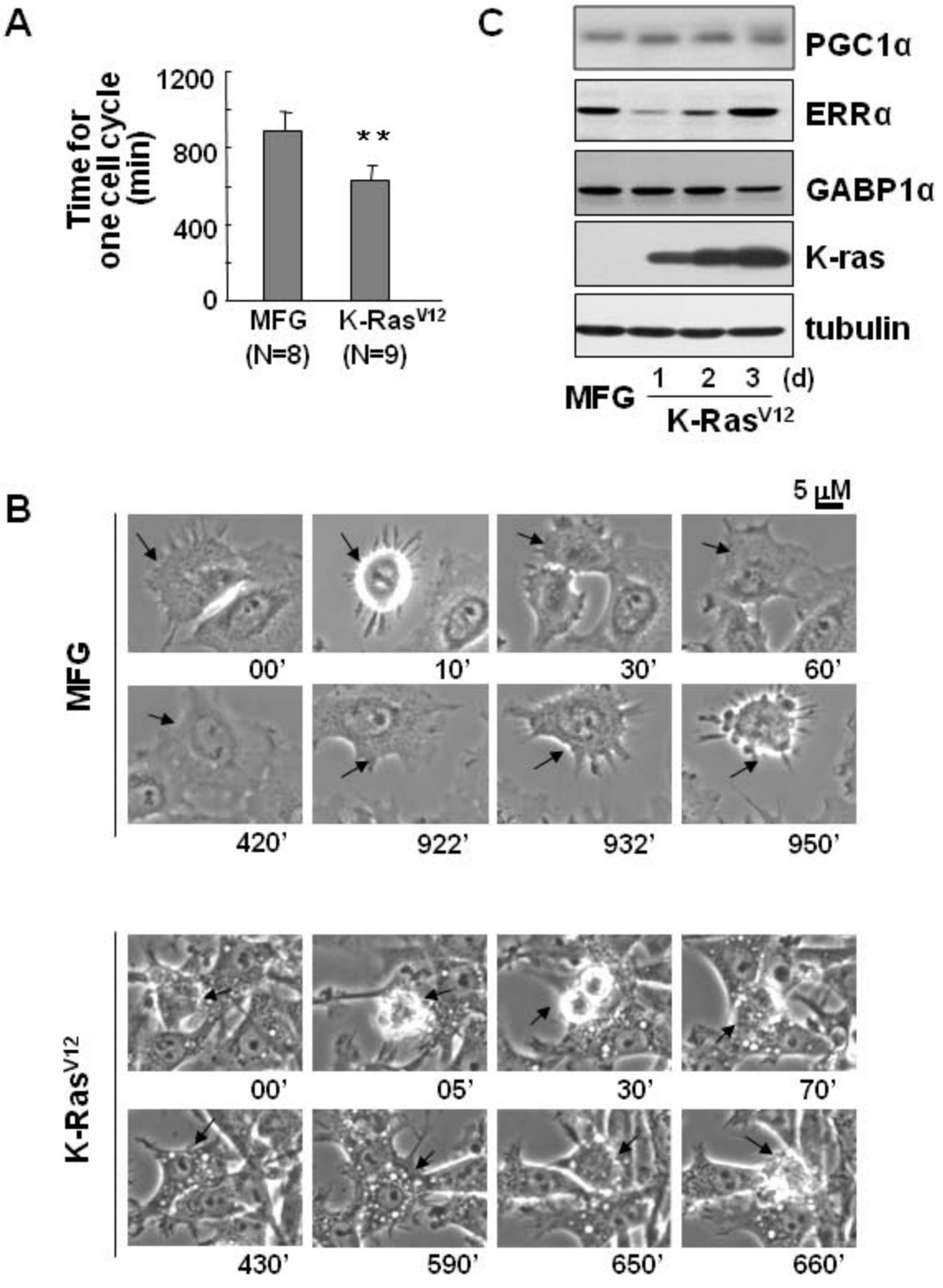

Supplementary Figure S3

Up-expressed genes

1. XM_575782	**ATPase, H+ transporting, Vo subunit D**
2. BC074011	**beclin1**
3. NM_019359	calponin 3, acidic
4. XM_216034	CDKN1A interacting Zf protein 1
5. NM_053354	Cyt-5-methyltransferase 1
6. BC060564	H2A histone family
7. NM_206847	phosphofructokinase
8. NM_022922	triosephosphate isomerase 1
9. XM_215416	pyrophosphatase
10. NM_012949	enolase 3, beta
11. NM_012580	heme oxygenase 1
12. BC081928	vaccinia related kinase 3
13. XM_213624	Mak3 homolog
14. NM_030867	nuclear factor of kappa light chain
15. XM_237999	Gadd45 gamma
16. M99252	osteopontin
17. NM_053883	dual specificity phosphatase 6
18. XM_342949	ribosomal protein L11
19. NM_019356	translation initiation factor 2 subunit 1 alpha
20. XM_575396	testis derived transcript
21. BC060548	putative ISG12(a) protein
22. BC083790	Uncharacterized gene
23. NM_199090	Uncharacterized gene
24. CF115498	Uncharacterized gene

Down-expressed genes

1. XM_341957	interferon induced transmembrane protein 3
2. XM_213484	vesicle amine transport protein 1
3. BC087063	cell division cycle associated 2
4. AJ005394	collagen alpha1 type V
5. BC061777	secreted acidic cystein rich glycoprotein
6. XM_213440	collagen alpha type 1
7. NM_019143	fibronectin 1
8. NM_053598	nudix-type motif 4
9. NM_031970	heat shock 27kDa protein 1
10. BC083876	pleckstrin homology containing, family C member 1
11. XM_213849	nuclear factor I/X
12. NM_139398	RNA helicase
13. NM_031099	ribosomal protein L5
14. BQ210711	Uncharacterized gene
15. AI454608	Uncharacterized gene
16. BI295306	Uncharacterized gene
17. CB327868	Uncharacterized gene
18. CN541734	Uncharacterized gene
19. CF111629	Uncharacterized gene
20. BC089991	Uncharacterized gene
21. CK839196	Uncharacterized gene

Supplementary Figure S4

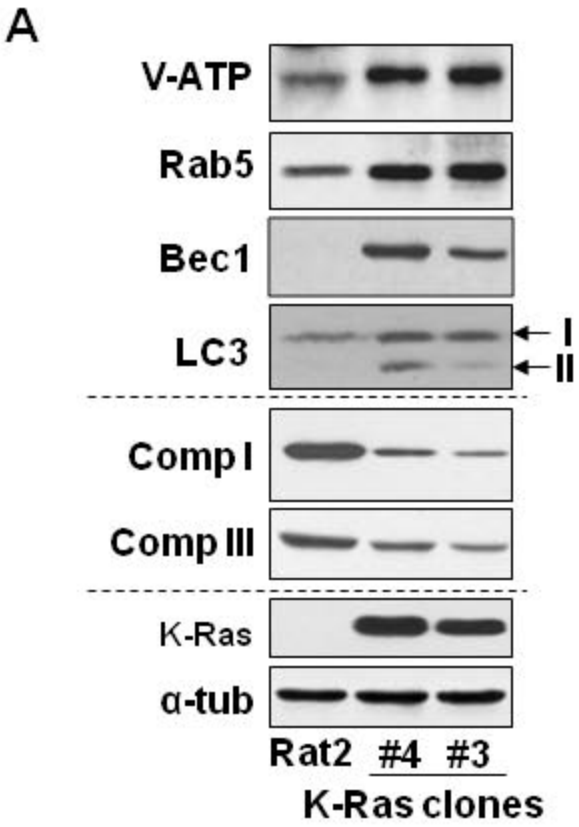

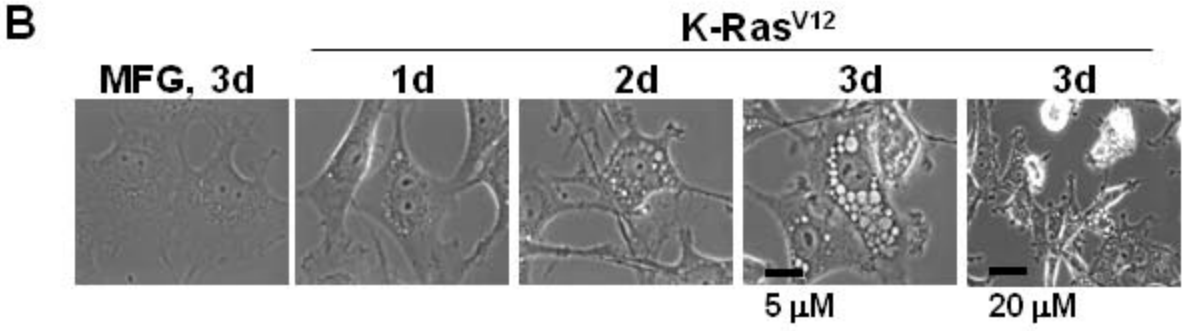

Supplementary Figure S5

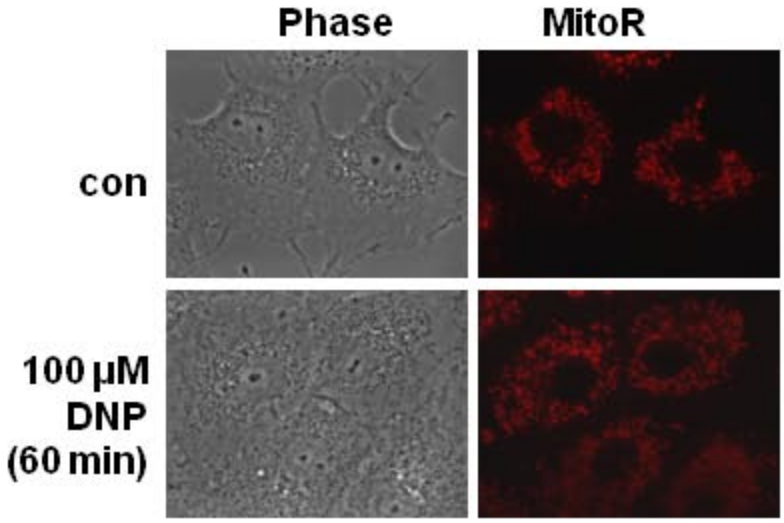

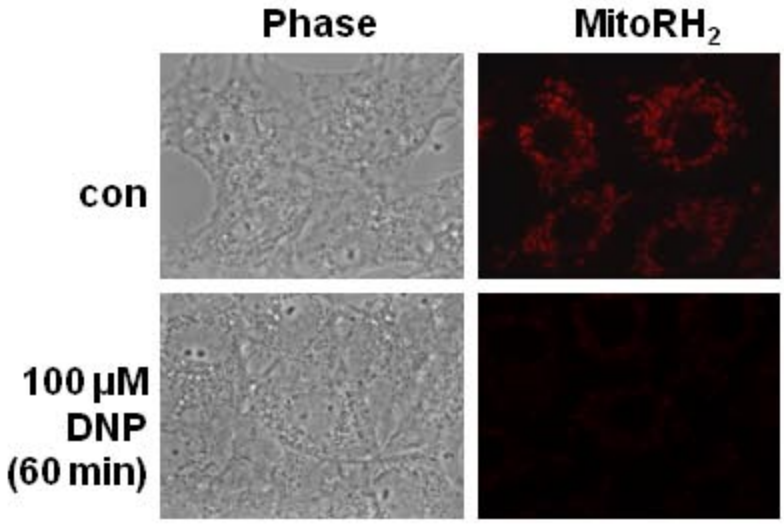

Supplementary Figure S6

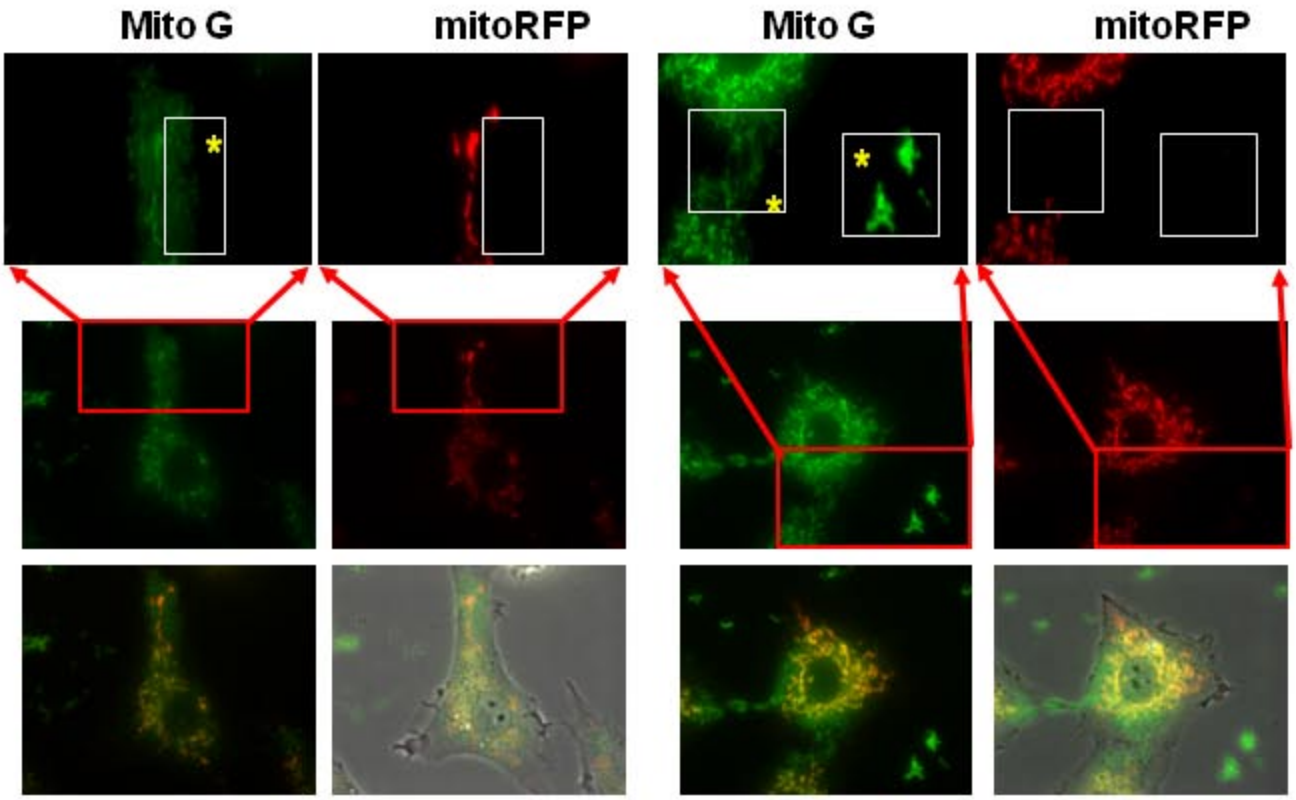

Supplementary Figure S7

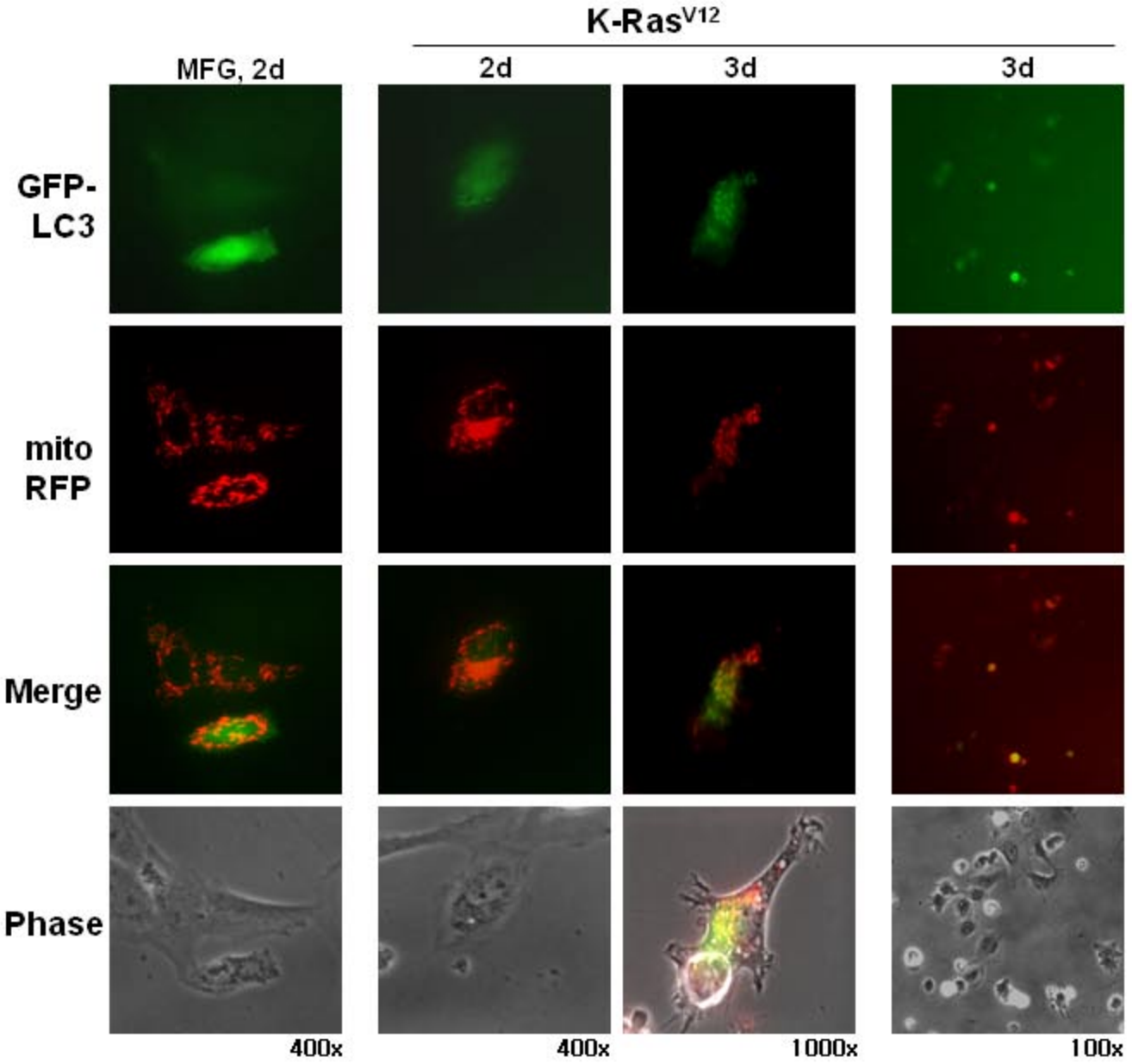

Supplementary Figure S8

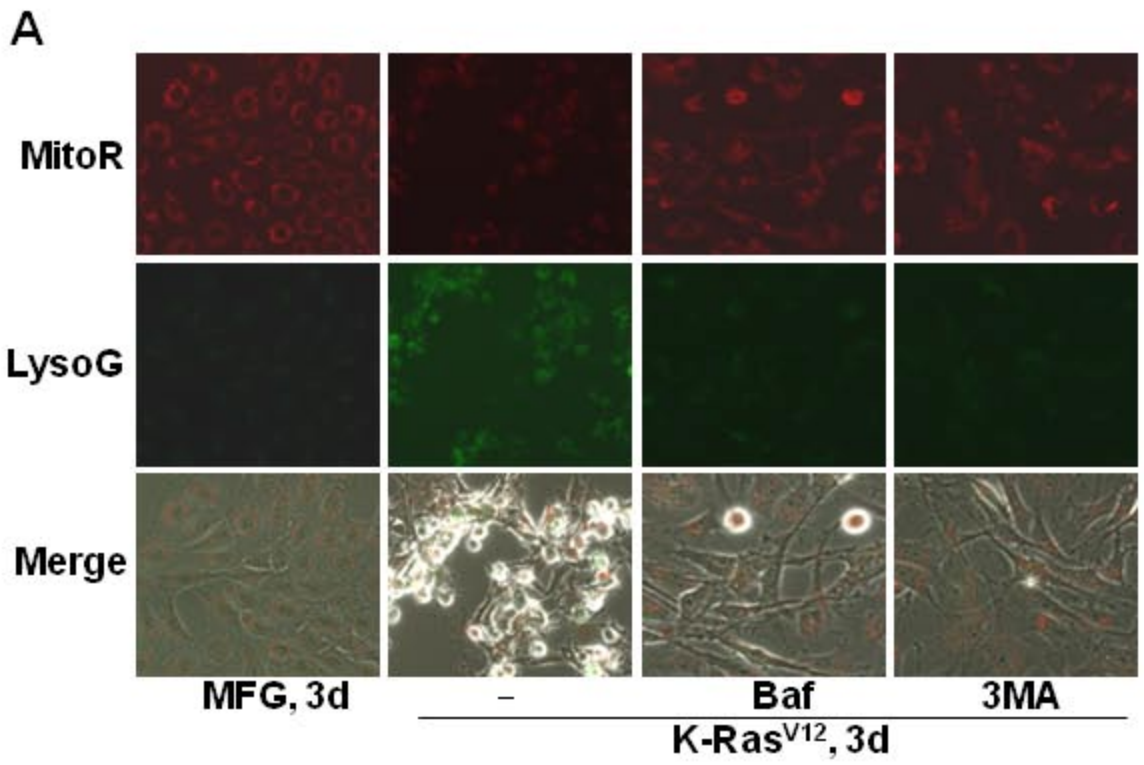

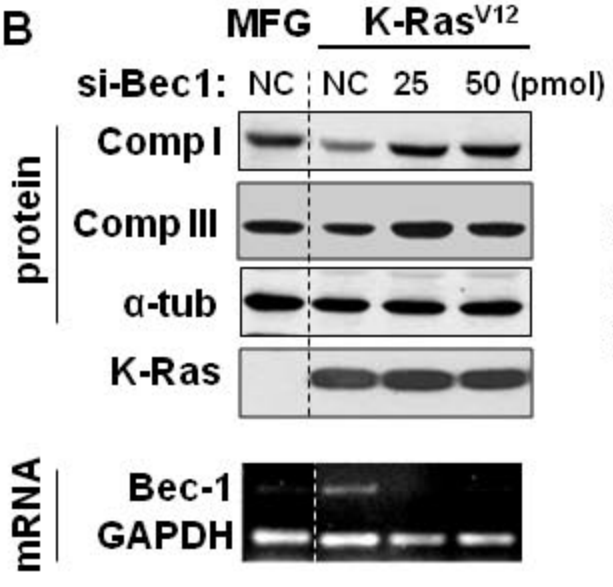

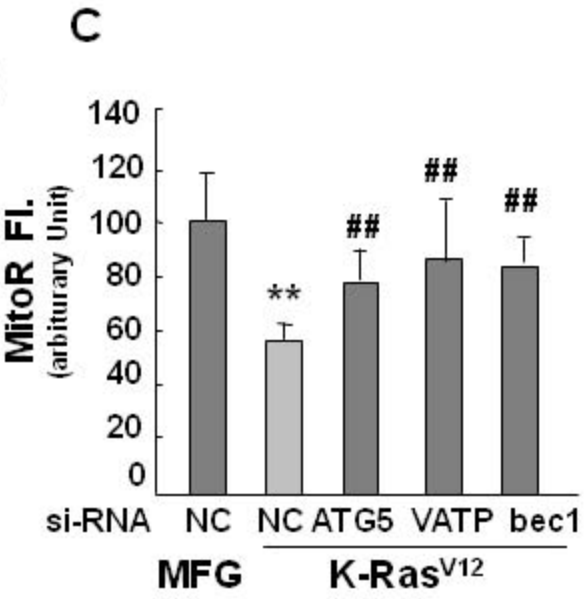

Supplementary Figure S9

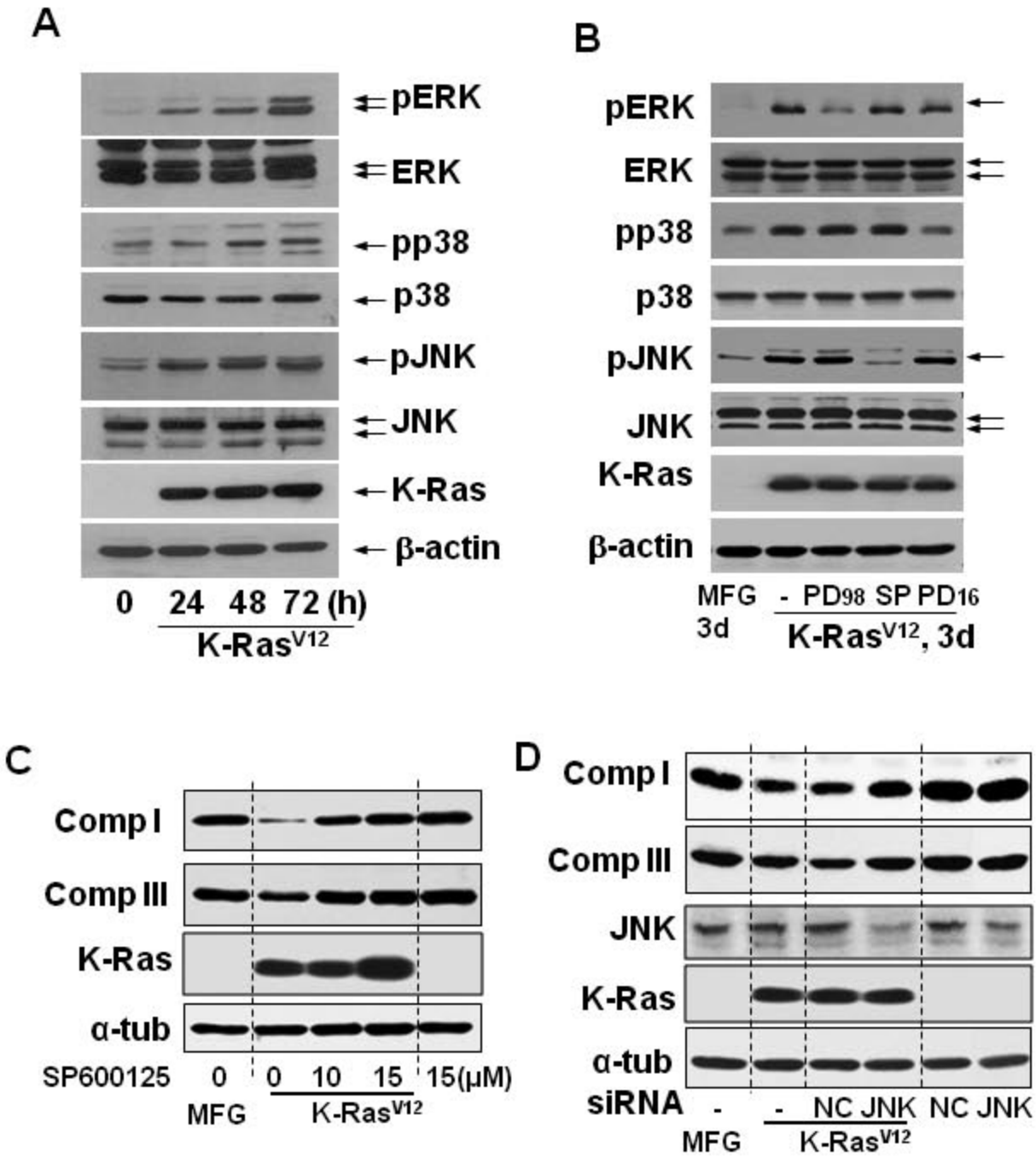

Supplementary Figure S10

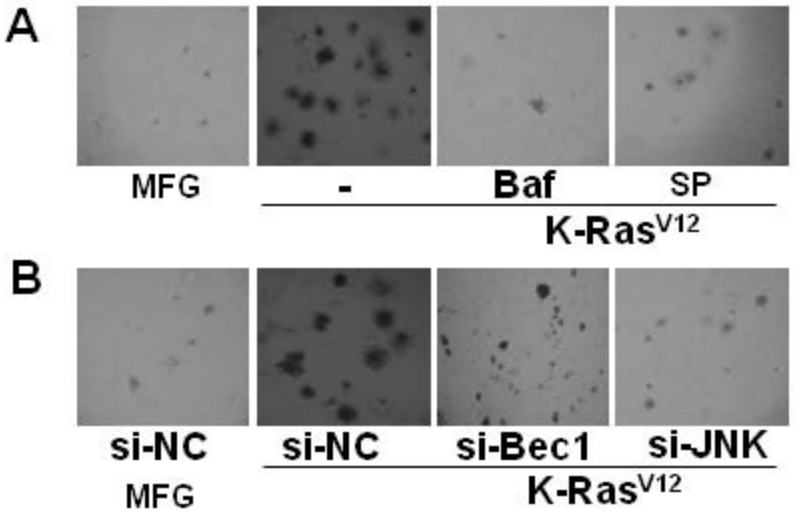

Supplementary Figure S11

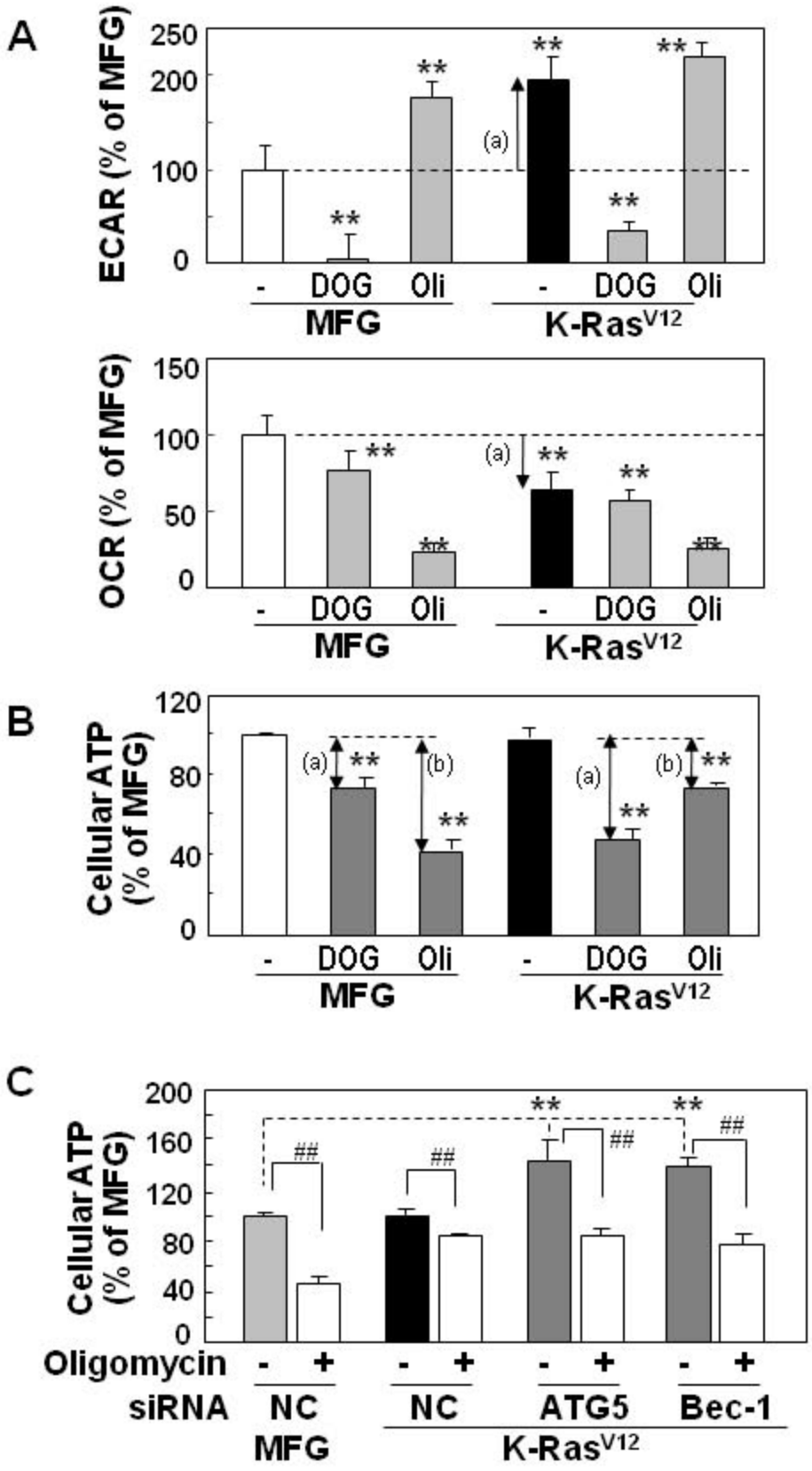

Figure Legends for Supplementary Figures

Supplementary Fig. S1. Cell morphology and viability of K-Ras^{V12}–infected Rat2 cells. Rat2 cells were infected with the indicated volumes of retrovirus harboring K-Ras^{V12} for the indicated periods. **(A)** Cell morphology was visualized with phase-contrast images. **(B)** Representative pattern of maximum oxygen consumption rate using Mitocell equipped with Clark oxygen electrode (782 Oxygen Meter). **(C)** Western blot analysis. **(D)** Cell viability was assessed by the LIVE/DEAD cell viability assay. The cells were continuously cultured for 5 day after infection with K-Ras^{V12} retrovirus. Green fluorescence (calcein AM, Cal-AM) indicates live cells and red fluorescence (ethidium homodimer, EthD) means dead cells. Dead cell treated by mitochondrial complex II inhibitor, 2-theonyltrifluoroacetone (TTFA) was used as control for EthD positive. K-Ras^{V12}-infected cells continuously grow and become aggregated whereas control Rat2 cells infected by MFG mock virus grow only in a monolayer, showing their loss of contact inhibition property by K-Ras^{V12}.

Supplementary Fig. S2. Time-lapse images of the K-Ras^{V12}-infected cells for one cell cycle progression and protein expressions of mitochondrial biogenesis regulators. Time-lapse images acquired at 1 min intervals were analyzed to estimate the time for one cell cycle progression. **(A)** Time for one cell cycle progression was estimated. The time required for one cell division was significantly shortened in K-Ras^{V12}-treated cells (11.6 ± 1.2 h), compared to control (16.8 ± 4.2 h). **(B)** Representative images for complete one cell division (from the point of cell detachment for mitosis outset to the point of re-detachment of the progeny for next mitosis) were shown. Arrows indicate the cells under being monitored. **(C)** Protein expressions of mitochondrial biogenesis regulators of Rat2 cells transiently infected by K-Ras^{V12}.

Supplementary Fig. S3. Differentially expressed genes by K-Ras^{V12} over-expression. Rat2 cells were infected with retrovirus harboring K-Ras^{V12} for 1 and 3 days. Total RNAs were extracted from the cells and reverse transcription was performed against the RNAs using 10 μM dT-ACP1 (5'-CGTGAATGCTGCGACTACGATIIIIIT(18)-3' and Moloney murine leukemia virus reverse transcriptase (200 U). First-strand cDNAs were applied to GeneFishing^{TM} Kit (Seegene, Seoul, South Korea) according to the protocol provided. Differentially expressed genes by K-Ras^{V12} were screened by ACP-based PCR method and persistently regulated genes in both cells infected for 1day and 3 days

were selected for directing sequencing. 50 sequenced genes (24 up-regulated and 21 down-regulated genes) are presented.

Supplementary Fig. S4. Protein expression profile of Rat2 cells stably expressing K-Ras^{V12} by Western blot analysis **(A)**, and time-course changes of cell morphology of Rat2 cells transiently infected by K-Ras^{V12} **(B)**.

Supplementary Fig. S5. Differential dependency of two different mitochondria-targeting fluorescent dyes on mitochondrial membrane potential. Rat2 cells were treated with 100 μM 2,4-dinitrophenol (Sigma-Aldrich) for 60 min and stained with 200 nM CMXRos (MitoR, Molecular Probe, M-7512) or 200 nM CMH_2XRos ($MitoRH_2$, Molecular Probe, M7513) for 10 min and visualized with Axiovert 200M fluorescence microscopy.

Supplementary Fig. S6. Non-specific targeting of MitoTracker Green to cell membrane or cell debris. Rat2 cells expressing mitochondria-targeting RFP (mitoRFP) were stained with 200 nM MitoTracker Green (Molecular Probe, M7514) and visualized with Axiovert 200M fluorescence microscopy. MitoTracker Green was targeted nonspecifically to cellular debris of plasma membrane even after washing twice with PBS (indicated with box).

Supplementary Fig. S7. Effect of K-Ras^{V12} on Rat2 cells expressing GFP-LC3. Rat2 cells were transfected with the two plasmids encoding GFP-LC3 and mitoRFP 18 h prior to K-Ras^{V12} infection and fluorescence images were taken. Most Rat2 cells expressing GFP-LC3 were dead after infection with K-Ras^{V12} retrovirus, implying that well balanced control between anti-death signal and autophagy activation by K-Ras is important.

Supplementary Fig. S8. Recovery of mitochondria by blocking autophagy. **(A)** Rat2 cells were exposed to bafilomycin A (1 nM) or 3MA (3 mM) 1 h prior to K-Ras^{V12} infection, and further incubated for 3 days. Then, cells were co-stained with 50 nM LysoTracker Green and 200 nM MitoTracker Red without fixation to visualize changes of mitochondrial and lysosomal mass with fluorescence microscopy. Images with 200x magnification are presented. Green indicates lysosomes and red indicates mitochondria. **(B)** Rat2 cells were transfected with siRNA for beclin-1 (si-beclin-1) 15 h prior to K-Ras^{V12} infection, and further incubated for 3 days. Expression of respiratory protein was

monitored by Western blot (upper three panels) and mRNA level of beclin-1 was estimated by RT-PCR (lower panel). **(C)** Mitochondrial mass was estimated as described in 'Materials and methods' after Rat2 cells were transfected with si-ATG5, si-VATPaseE, and si-beclin-1 15 h prior to K-Ras^{V12} infection, and further incubated for 3 days. **, $p<0.01$ vs. MFG (si-NC) control and $^{\#\#}$, $p<0.01$ vs. K-Ras-infected (si-NC) cells by one-way ANOVA.

Supplementary Fig. S9. K-Ras^{V12}-induced autophagy is mediated through JNK. **(A)** Rat2 cells were infected with retrovirus harboring K-Ras^{V12} for the indicated periods. Phosphorylation status of MAPKs (ERK, p38, and JNK) was monitored by Western blot analysis. **(B)** Western blot analysis. Rat2 cells were exposed to pharmacological inhibitors (15 μM PD98059, 15 μM SP600125, or 15 μM PD169316) prior to K-Ras^{V12} infection and further incubated for 3 days as indicated. **(C, D)** Western blot analysis. Rat2 cells were exposed to SP600125 or transfection of si-RNAs (si-NC, si-beclin-1, si-JNK) prior to K-Ras^{V12} infection and further incubated for 3 days.

Supplementary Fig. S10. Blocking autophagy inhibits K-Ras^{V12}-induced cell transformation. Rat2 cells were exposed to pharmacological inhibitors (15 μM SP600125 or 1 nM Bafilomycin A) or transfection of si-RNAs (si-NC, si-beclin-1, si-JNK) prior to K-Ras^{V12} infection and soft-agar colony forming assay was performed.

Supplementary Fig. S11. Metabolic alteration by K-Ras. **A-B**, After infected by K-Ras^{V12} retrovirus for 3 days, Rat2 cells were treated with 2 μM oligomycin (Oli) or 25 mM 2-deoxyglucose (DOG) for 3 h. **(A)** Extracellular acidification rate (ECAR) and cellular oxygen consumption rate (OCR) were simultaneously measured by Seahorse XF analyzer as described in 'Materials and Methods.' (a) indicates changes by K-Ras. **(B)** Intracellular ATP levels. DOG-sensitive (glycolysis dependent) and Oli-sensitive (mitochondrial respiration dependent) ATP production are indicated as (a) and (b), respectively. **(C)** Intracellular ATP levels. Rat2 cells were transfected with si-ATG5 or si-Beclin-1 (Bec-1) 15 h prior to K-Ras^{V12} infection and further incubated for 3 days, then treated with 2 μM oligomycin for 3 h.